DOI: 10.1002/ejic.200700047

Structural Chemistry of an $n = 1$ Member of the Ruddlesden–Popper $Sr_{n+1}(Co_{0.5}Ta_{0.5})_nO_{3n+1}$ Homologous Series: Sr_4CoTaO_8

Khalid Boulahya,[a] Marina Parras,[a] and José María González-Calbet*[a]

Keywords: Electron diffraction / X-ray diffraction / Electron microscopy / Magnetic properties

A layered perovskite related compound with the Sr_4CoTaO_8 composition was isolated. This material constitutes the $n = 1$ member of the recently reported $[Sr_{n+1}(Co_{0.5}Ta_{0.5})_nO_{3n+1}]$ Ruddlesden–Popper series. XRPD, SAED and HREM reveal that this compound crystallizes as a K_2NiF_4-type with space group $I4/mmm$. The structure is formed by one Sr_2CoTaO_6 perovskite block that intergrows with one SrO rock salt layer; no ordering between the Co and Ta cations was established.

Introduction

Main-layered perovskites and their derivatives are characterized by an excess of anions relative to the ideal perovskite, and they constitute homologous series that are defined on the basis of the interslab composition and orientation of the layer plane relative to the aristotype cubic lattice. When this layer is parallel to the (001) plane of the cubic perovskite, the $(ABO_3)_nAO$ Ruddlesden–Popper (RP) series[1] arises. Most of the RP phases described up to now contain B cations of the first transition series, such as Ti, Ni, Cu, ...; however, structures related to the $n = 2$ member of this series, $Sr_3Co_2O_{7-\delta}$, which involves the substitution of Co by other metals of the later transition series, have been recently reported.[2] Indeed, a broad range of complex tantalum oxides have been reported to exhibit very high photocatalytic activities for the decomposition of water into H_2 and O_2; this is one of the most promising pathways for the conversion of photon energy into chemical energy.[3] For instance, $A_2SrTa_2O_7$ (A = H, K, Rb)[4] is the $n = 2$ member of the RP-layered series whose structure is built up of two cubic perovskite blocks that intergrow with a SrO rock-salt-type layer. The substitution of a monovalent cation by a divalent cation in the A sublattice must be accompanied by the partial substitution of Ta by other metals that stabilize lower oxidation states. In an attempt to stabilize homologous series with cations of later transition-metal series, and taking into account the versatility of cobalt, we recently isolated the $n = 2$ and $n = \infty$ members of the $Sr_{n+1}(CoTa)_nO_{3n+1}$[5] family with a Co/Ta ratio of 1:1.

Cobalt-containing systems present a particular behaviour when compared with other RP series, and this difference in behaviour is related to the difficulty in stabilizing the $n = 1$ term. In fact, Sr_2CoO_4 can only be stabilized under high pressure conditions[6] whereas the upper n terms can be easily prepared under atmospheric pressure. In a somewhat similar way, the high temperatures used to stabilize the different members of the $Sr_{n+1}(CoTa)_nO_{3n+1}$ series were not adequate to isolate the first member ($n = 1$) because disordered intergrowths of upper members ($n > 1$) were usually obtained. Lower synthetic temperatures combined with longer annealing times allowed us to successfully stabilize, for the first time, this $n = 1$ member. In this paper, we describe the synthetic conditions and microstructural characterization of the $n = 1$ member of this series, which possesses the composition $Sr_2(Co_{0.5}Ta_{0.5})O_4$ (i.e. Sr_4CoTaO_8). This is the end, in the absence of tilting, members of the series belong to the $I4/mmm$ K_2NiF_4 structural type with the layer sequence (ABO_3) perovskite-(AO) rock salt. To fully determine the structural details and physical properties of the series, X-ray powder diffraction (XRPD), selected area electron diffraction (SAED), high resolution electron microscopy (HREM) and magnetic properties were investigated.

Results and Discussion

The synthetic pathway to Sr_4CoTaO_8 was followed by XRPD. After annealing for three days, the XRPD pattern can be indexed on the basis of a single A_2BO_4, $n = 1$ RP single phase. As it is well known, different members of the RP series ranging from $n = 1$ to $n = \infty$ (the ABO_3 perovskite structure) can be isolated. However, the presence of disorder in the stacking of the perovskite and SrO blocks is not unusual and it is not always detected by powder X-ray diffraction, and therefore, careful microstructural study of these phases is always advisable. In fact, the microstructural study of Sr_4CoTaO_8 by HREM confirms that most of the

[a] Departamento de Química Inorgánica, Facultad de Químicas, Universidad Complutense de Madrid
28040 Madrid, Spain
Fax: +34-91-394-4352
E-mail: jgcalbet@quim.ucm.es

crystals are constituted by intergrowth of $n = 1$ and $n = \infty$ members of the RP series.

Actually, in the [010] zone image (Figure 1), $n = 1$ regions, A_2BO_4 structural blocks intergrow with isolated lamellae of the cubic perovskite $n = \infty$ member of the mentioned series. Moreover, in some crystals, the intergrowth of the $n = 1$ member with other related superstructures, which correspond to other terms of the RP series, is apparent. The presence of this type of disorder was attributed to kinetic reasons. In fact, sintering times play an important role in the stabilization of single phases and, usually, long times are necessary to avoid intergrowths of different members of the series. Therefore, to attain a long range ordered material, the sample was reannealed. After seven days at 1000 °C, a fully ordered Sr_4CoTaO_8 single phase was isolated as revealed by XRPD, SAED and HREM.

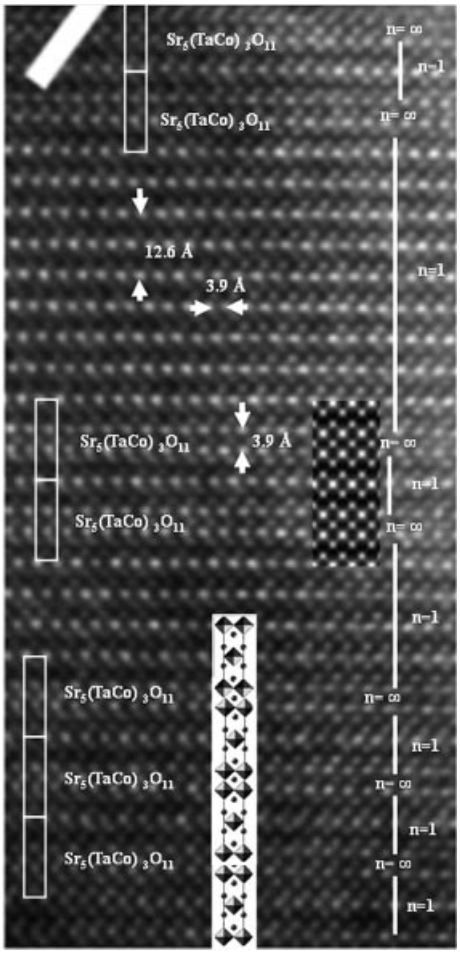

Figure 1. HRTEM image along the [010] zone axis that corresponds to a sample with nominal composition Sr_4CoTaO_8 after 3 d annealing. $Sr_5(CoTa)_3O_{11}$ ($n = 1.5$) member of $Sr_{n+1}(Co_{0.5}Ta_{0.5})_nO_{3n+1}$ series intergrows in a disordered way with $n = 1$ regions. Ideal structural model of $Sr_5(CoTa)_3O_{11}$ and calculated image from the model are shown in the inset.

The whole XRPD pattern (Figure 2) can be indexed on the basis of a tetragonal unit cell with lattice parameters $a = b = 3.8991(1)$ and $c = 12.6264(8)$ Å, no extra reflections are detected. SAED was used to fully reconstruct the reciprocal space. The most relevant zone axes, [001] and [010], are depicted in Figure 3. The diffraction spots are always sharp; streaking or diffuse intensity, which are indicative of some disorder, are not observed. All reflections can be indexed on the basis of the above tetragonal unit cell. Besides, the reflection conditions are compatible with the *I*4/*mmm* (139) space group, which was previously proposed for other $n = 1$ members of the RP family.[9]

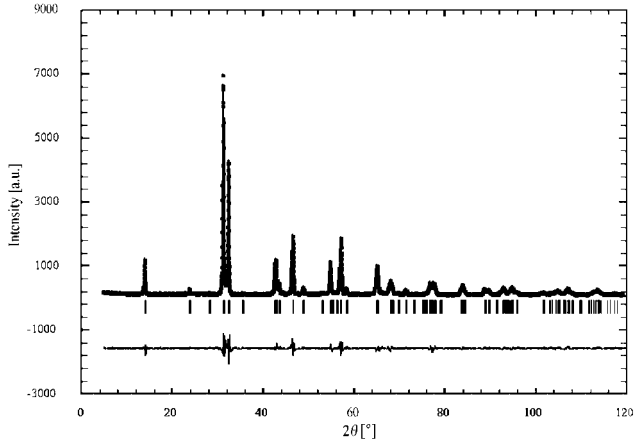

Figure 2. Graphic results of the fitting of the XRPD powder data of Sr_4CoTaO_8: experimental (points), calculated (solid line) and difference (bottom).

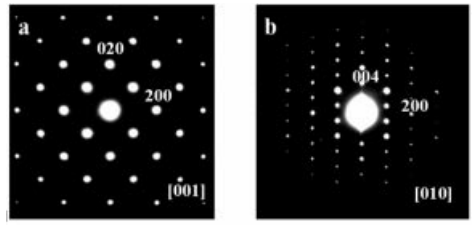

Figure 3. SAED patterns corresponding to Sr_4CoTaO_8 along (a) [001] and (b) [010] zone axes.

The [010] HREM image (Figure 4) corresponds to an apparently well-ordered material that shows *d*-spacing of 3.9 Å and 12.6 Å, which corresponds to d_{100} and d_{001}, respectively. The contrast variation in this image corresponds to two layers with black dots that are marked by an arrow, which can be associated to Sr atoms of the rock salt blocks; these layers are separated by one layer with less intense dots that are marked by a dashed arrow, which correspond to Co/Ta atoms of the perovskite blocks. This configuration is shown in the enlarged image of Figure 4 and corresponds to the structural model depicted in Figure 5. Fourier transform was performed on the HREM micrograph to look for the existence of different domains that could indicate the presence of additional Co/Ta ordering in the structure. However, the whole crystal is homogeneous and no additional ordering was observed. Therefore, from the corresponding ideal atomic coordinates, an image calculation was performed. The simulated image fits nicely to the experimental one for $\Delta f = -50$ nm and $\Delta t = 6$ nm (see Figure 4).

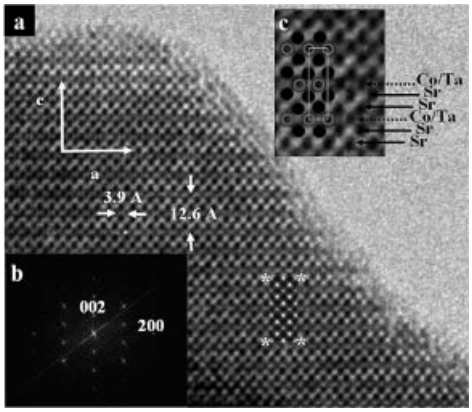

Figure 4. (a) HRTEM image of Sr_4CoTaO_8 along the [010] zone axis. Calculated image is shown in the inset. (b) Corresponding optical Fourier transform (FT). (c) Image magnification where metal atoms are superimposed.

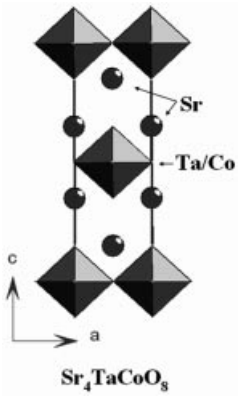

Figure 5. Structural model of Sr_4CoTaO_8 along the *b* axis.

B-site ordering for Co compounds has only been reported in K_2NiF_4-related materials when monovalent and trivalent cations occupy this site. For instance, Abou-Warda et al.[10] suggest that ordering of Co and Li in $La_2Li_{0.5}Co_{0.5}O_4$ is due to size rather than charge differences [$^{VI}r_{Li^+}$ = 0.76 Å; $^{VI}r_{Co^{3+}}$ = 0.545 Å (low-spin)]. In our case, the smaller difference between the Co^{3+} and Ta^{5+} radii ($^{VI}r_{Ta^{5+}}$ = 0.76 Å) could justify the disorder between the $[CoO]_6$ and $[TaO]_6$ octahedra.

According to the above results, an X-ray profile refinement of Sr_4CoTaO_8 was performed. The structure was solved in the *I*4/*mmm* space group by taking the crystallographic data corresponding to an n = 1 member of this layered family as a starting point.[11] Because no evidence for the presence of Co/Ta order in the B sublattice was detected, both cations were randomly distributed over the octahedral sites in a first stage. Peak shapes were described by pseudo-Voigt functions. Figure 2 shows the graphic results of the fitting of the experimental X-ray diffraction pattern and the difference between observed and calculated data. The refinement was stable, and it was possible to refine the positions of the oxygen atoms provided that a temperature factor for each type of atom was used. Structure refinement confirms isotypism with Sr_2TiO_4.[11] The final structural parameters are collected in Table 1, and Table 2 shows some selected interatomic distances.

Table 1. Final structural parameters of Sr_4CoTaO_8.[a]

Atom	*x*/*a*	*y*/*b*	*z*/*c*	B_{iso}	*Occ*
Sr1	0.50000	0.5000	01466(1)	1.68(4)	1.00000
Ta/Co1	0.00000	0.00000	0.00000	1.53(5)	1.00000
O1	0.50000	0.00000	0.00000	1.85(13)	1.00000
O2	0.00000	0.00000	0.1684(8)	1.85(13)	1.00000

[a] S.G. *I*4/*mmm* (139), a = 3.8991(1) Å, a = 12.6264(8) Å, V = 191.962(2) Å^3. R_{wp} = 0.118, R_{exp} = 0.070, R_B = 0.038, χ^2 = 2.6.

Table 2. Selected interatomic distances [Å] in Sr_4CoTaO_8.

Sr1–O1: 2.688(1) × 4	Co/Ta–O1: 1.950(0) × 4
Sr1–O2: 2.336(1)	Co/Ta–O2: 2.126(1) × 2
Sr1–O2: 2.771(1) × 4	

Refinement of the XRPD pattern confirms that Sr_4TaCoO_8 constitutes a new example of an n = 1 term of the layered RP family. The structure consists of layers of corner-sharing $[Co/TaO_6]$ octahedra running perpendicular to the *c* axis and separated by Sr atoms. Adjacent sets of layers are staggered as shown in Figure 5. The observed Co/Ta–O(1) and Co/Ta–O(2) bond lengths of 1.950(0) and 2.126(1) Å indicate that the octahedra are tetragonally distorted along the *c* axis. These interatomic Co/Ta–O distances fit well with those of analogous oxides as $K_2SrTa_2O_7$[12] [distances Ta–O, 2.102(1)–1.812(1) Å] or $Sr_3Co_2O_{7-\delta}$[2] where the Co–O interatomic distances range from 1.92 to 2.00(1) Å. Finally, the Sr–O [2.771(1)–2.336(1) Å] distances are similar to those observed in other Sr oxides. At this point, it is worth remembering that the analogous Sr_2CoO_4 phase is only stabilized under high pressure. The partial substitution of Co by Ta^V reduces the oxidation state of Co from IV to III in Sr_4CoTaO_8, which allows their stabilization under ambient pressure.

Figure 6 shows the temperature dependence of the magnetic susceptibility for Sr_4CoTaO_8 in the temperature range from 150 to 300 K. Sr_4CoTaO_8 exhibits a small and flat

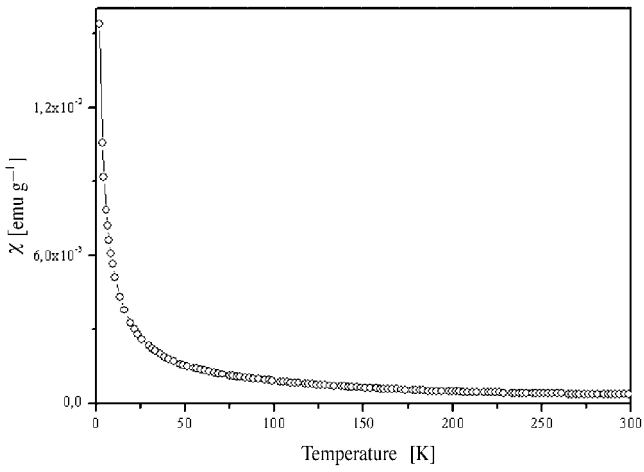

Figure 6. Magnetic susceptibility versus temperature plot corresponding to Sr_4CoTaO_8.

susceptibility, with a significant increase only at low temperatures. This low-temperature tail is usually attributed to spurious local paramagnetic moments. A similar behaviour was reported for $NaCoO_2$,[13] with all Co as low spin Co^{III}.

Conclusions

The $n = 1$ member of the $[Sr_{n+1}(Co_{0.5}Ta_{0.5})_nO_{3n+1}]$ Ruddlesden–Popper series was successfully isolated. Large annealing times were necessary because SAED and HREM show that the first stage of the synthesis of Sr_4CoTaO_8 requires the initial formation of intergrowths of different members of the series. In this case, Sr_4CoTaO_8 intergrowths with the $n = \infty$ term is observed in most of the crystals.

A very interesting point of this work arises from this result. From the micrograph shown in Figure 1 it is clear that the existence of a new stable term of the series, formed by the ordered stacks of one Sr_4CoTaO_8 and one $SrCo_{0.5}Ta_{0.5}O_3$ structural block is possible and this corresponds to a chemical composition of $Sr_5(Co_{0.5}Ta_{0.5})_3O_{11}$. This recurrent intergrowth constitutes the $n = 1.5$ term, and this is the first example of a noninteger member of a RP series. This result opens the route to the research of new members of this series. We are currently investigating the synthetic conditions necessary to stabilize this new series member, and we hope to publish the results of this study in the near future.

Experimental Section

Polycrystalline Sr_4CoTaO_8 was synthesized by heating stoichiometric amounts of $SrCO_3$ (Aldrich 99.98%), Co_3O_4 (Aldrich 99.9%) and Ta_2O_5 (Aldrich 99+%) at 1000 °C for 7 d. Annealing at higher temperatures does not lead to an ordered situation. In fact, the microstructural study shows that most parts of the crystals are constituted by disordered intergrowths of different members of the RP series, which results from the loss of SrO layers. X-ray powder diffraction (XRPD) patterns were collected by using Cu-K_α radiation (λ = 1.5418 Å) at room temperature with a PHILIPS X'PERT diffractometer equipped with a graphite monochromator. Diffraction data were analyzed by the Rietveld method[7] with the use of the Fullprof program.[8] The sample was characterized by selected area electron diffraction (SAED) and high resolution electron microscopy (HREM) with a JEOL 3000 FEG electron microscope, fitted with a double tilting goniometer stage (±20°, ±20°). Local composition was analyzed by energy-dispersive X-ray spectroscopy (EDS) with an Oxford analyzer system attached to the above-described electron microscope. Magnetization was measured with a SQUID Quantum Design MPMS magnetometer, in a temperature range from 2 to 300 K, and magnetic field of 1000 Oe.

Acknowledgments

Financial support through research projects MAT2004-01248, MAT/0627/2004 and CAM/S-0505/PPQ0316 is acknowledged. K. B. thanks the MCYT (Spain) for financial support under the "Ramón y Cajal" Program.

[1] S. N. Ruddlesden, P. Popper, *Acta Crystallogr.* **1958**, *11*, 54–55.
[2] S. E. Dann, M. T. Weller, *J. Solid State Chem.* **1995**, *115*, 499–507.
[3] K. Domen, J. N. Kondo, M. Hara, T. Takata, *Bull. Chem. Soc. Jpn.* **2000**, *73*, 1307–1331.
[4] K. Shimizu, Y. Tsuji, T. Hatamachi, K. Toda, T. Kodama, M. Sato, Y. Kitayama, *Phys. Chem. Chem. Phys.* **2004**, *6*, 1064–1069.
[5] K. Boulahya, M. Parras, J. M. González-Calbet, *Chem. Eur. J.* **2007**, *13*, 910–915.
[6] X. L. Wang, E. Takayama-Muromachi, *Phys. Rev. B* **2005**, *72*, 064401(1–7).
[7] H. V. Rietveld, *Appl. Crystallogr.* **1969**, *2*, 65–71.
[8] J. Rodríguez-Carvajal, *Physica* **1993**, *B192*, 55–69.
[9] P. Ganguly, C. N. R. Rao, *J. Solid State Chem.* **1984**, *53*, 193–216.
[10] S. Abou-Warda, W. Pietzuch, G. Berghöfer, U. Kesper, W. Massa, D. Reinen, *J. Solid State Chem.* **1998**, *138*, 18–31.
[11] S. N. Ruddlesden, P. Popper, *Acta Crystallogr.* **1957**, *10*, 538–539.
[12] T. A. Kodenkandath, J. B. Wiley, *Mater. Res. Bull.* **2000**, *35*, 1737–1742.
[13] G. Lang, J. Bobroff, H. Alloul, P. Mendels, N. Blanchard, G. Collin, *Phys. Rev. B* **2005**, *72*, 094404 (1–7).

Received: January 15, 2007
Published Online: March 28, 2007

